

Muon transfer from hydrogen to argon and helium at 10–15 bars

R. Jacot-Guillarmod, F. Bienz, M. Boschung, C. Piller, L. A. Schaller,
L. Schellenberg, and H. Schneuwly
Institut de Physique de l'Université, CH-1700 Fribourg, Switzerland

W. Reichart
Physikinstitut der Universität, CH-8001 Zürich, Switzerland

G. Torelli
Istituto di Fisica dell'Università and Istituto Nazionale di Fisica Nucleare, I-56000 Pisa, Italy
(Received 24 March 1988)

The transfer of negative muons from the ground state of muonic hydrogen to argon and helium has been measured in gaseous mixtures at pressures between 10 and 15 bars and at different relative concentrations. The transfer rate to argon, reduced to liquid-hydrogen density [$\Lambda_{pAr} = 1.42(4) \times 10^{11} \text{ s}^{-1}$], agrees well with those obtained at ten times higher pressures. The transfer rate to helium [$\Lambda_{pHe} = 0.88(9) \times 10^8 \text{ s}^{-1}$], measured in a triple gas mixture, disagrees with the only other experimental value and is about two times higher than recent theoretical predictions. In addition, the muonic x-ray intensities of the Lyman series of argon resulting from muon transfer have been determined. They are well reproduced by a cascade calculation assuming a theoretical initial distribution over n and l states.

I. INTRODUCTION

Since the first observation of a muon-catalyzed fusion reaction by Alvarez *et al.*,¹ a great number of experimental and theoretical studies have been published on muon processes in hydrogen isotopes and, in particular, on the formation of mesomolecules. The discovery of this fusion reaction and the observation of the resonant formation of mesomolecules² gave rise to speculations about the practical use of this reaction for nuclear energy production.³

In the fusion reaction of heavy hydrogen isotopes, helium nuclei are produced. In dd fusion, the probability that the muon sticks to the helium nucleus after the fusion reaction is 12.2(3)%.⁴ In dt fusion, the sticking probability is much lower, around 0.5%.^{5–7} In the latter case, the recycled muon would be able to catalyze ideally about 200 fusion reactions.⁸

The number of muon cycles is not only limited by the muon sticking to the fusion product, but also by the muon capture by helium and the muon transfer from a hydrogen isotope to helium nuclei. It is therefore important to test models and theoretical predictions relative to the last two processes. In a preceding work,⁹ we reported on muon transfer to argon at pressures of 100 and 140 bar and at different concentrations.

The present paper, where we use the same experimental techniques, reports on measurements of muon transfer from muonic hydrogen in the $1s$ state to argon and helium at pressures between 9.6 and 14.9 bar. For each mixture, the mean lifetime of the $(\mu p)_{1s}$ system and the transfer rate have been determined. In addition, the muonic argon K -series intensities due to transfer have been measured to study their dependence upon pressure

and relative concentration. The measured values are compared with cascade calculations starting with a theoretical muon population in (n, l) states.

II. PRESENT STATUS OF RESEARCH ON TRANSFER TO HELIUM

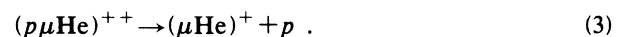
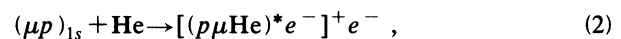
The first measurements of muon transfer from muonic hydrogen to helium^{10–13} seemed to confirm the very low transfer rate predicted in the first theoretical paper on transfer by Gershtein.¹⁴ The smallness of the predicted rate for the process



is due to the absence of crossing and pseudocrossing terms corresponding to charge exchange from the hydrogen K orbit.

Ten years later the calculation by Matveenko and Ponomarev,¹⁵ employing the perturbed stationary-state method, yielded a transfer rate which was five times greater than the quasiclassical estimate by Gershtein.

In 1981 Aristov *et al.*¹⁶ proposed a new mechanism for the muon transfer to helium, where, in an intermediate stage, a muonic molecule is produced in an excited state:



After deexcitation to the ground state, this molecule decays into a muonic helium atom and a hydrogen nucleus. The predicted rate (normalized to the atomic density of liquid hydrogen) at room temperature for the muon transfer from a thermalized $(\mu p)_{1s}$ atom to ^4He of $0.44 \times 10^8 \text{ s}^{-1}$ is about one order of magnitude greater

than that calculated by Matveenko and Ponomarev.

In their experiment using a triple gas mixture H_2 -He-Xe, Bystritskii *et al.*¹⁷ obtained, by analyzing the time structure of γ events, a muon transfer rate from hydrogen to helium of $0.36(10) \times 10^8 \text{ s}^{-1}$, in agreement with the prediction of Aristov *et al.*

Kravtsov *et al.*¹⁸ improved the calculation of Aristov *et al.* by taking into account the form factor of the molecular ion $[(p\mu\text{He})e^-]^+$ and the influence of the electron cloud of the target atom upon the energy levels and upon the rates of the $p\mu\text{He}$ -molecule formation. Depending on the approximations made in these calculations, the muon transfer rate from protium to ^4He at room temperature varies between 0.43×10^8 and $0.52 \times 10^8 \text{ s}^{-1}$. Using in addition the Hartree-Fock approximation for atomic wave functions, Ivanov *et al.*¹⁹ obtained lower rates for the $\mu p + ^4\text{He}$ charge-exchange reaction, i.e., values between 0.32×10^8 and $0.35 \times 10^8 \text{ s}^{-1}$. The agreement with experimental data of other charge-exchange reactions^{5,17,20,21} is satisfactory. It evidences the need for correctly taking into account the atomic shell in the calculation of bound states of muonic molecules.¹⁹

III. EXPERIMENTAL METHOD

At a pressure of a few atmospheres, the fate of a negative muon in a H_2 -He gas mixture, containing a small amount of argon, can be sketched as in Fig. 1. Just after its formation, the muonic hydrogen atom $(\mu p)^*$ has a kinetic energy between 0.1 eV (Ref. 22) and 1 eV.²³ In a recent experiment,²⁴ it has been observed that the kinetic energy distribution of $\pi^- p$ atoms just before the charge-

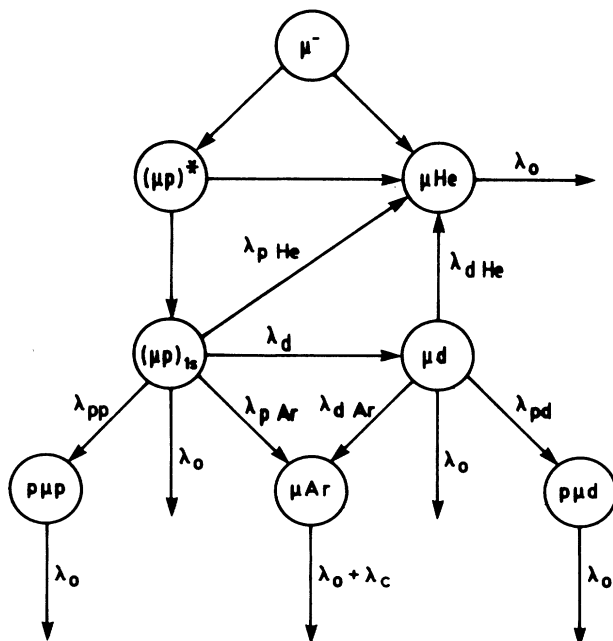


FIG. 1. Scheme of muonic capture in a mixture of hydrogen and helium with a small amount of argon. Only the main processes at 10 bars are shown.

exchange reaction has a component extending up to ~ 1 eV and a tail up to ~ 50 eV. By taking into account the Stark mixing, the muonic cascade in hydrogen can be correctly reproduced assuming capture in an atomic level around $n=14$ with statistical angular momentum distribution.^{20,25,26} The $(\mu p)^*$ atom deexcites step by step to the level $n=4$ essentially through external Auger effect on helium atoms and hydrogen molecules, through Coulomb deexcitation and molecular dissociation. At 10 atm, the $n=4$ level is reached in about 5×10^{-11} s. The further deexcitation down to the $1s$ ground state proceeds predominantly through radiative transitions in about 10^{-10} s.

The process of thermalization of μp atoms is not well known. However, even if the elastic scattering



which is the dominant process in the deceleration of μp atoms, has a small cross-section of the order of 10^{-20} – 10^{-19} cm^2 (Refs. 13 and 27–30) at kinetic energies between 0.04 and 1 eV, the major part of the μp atoms is thermalized after about ten collisions.³¹

In H_2 -Z gas mixtures, where the components have comparable concentrations, the transfer from excited $(\mu p)^*$ states is in competition with deexcitation processes. The corresponding transfer rates can only indirectly be determined, e.g., for pion transfer in binary gas mixtures.³²

If the relative atomic concentration of the Z atoms is small, i.e., $c_Z/c_p \ll 1$, the transfer of muons from μp atoms to Z atoms proceeds from the ground state of thermalized μp atoms.

Three processes contribute essentially to the disappearance rate of μp atoms in a H_2 -He-Ar gas mixture: (a) the free decay of the muon with a rate $\lambda_0 = 0.455 \times 10^6 \text{ s}^{-1}$, (b) the formation of $p\mu p$ molecules with a rate λ_{pp} , and (c) the transfer of the muon to argon (λ_{pAr}), to helium (λ_{pHe}), to deuterium (λ_d) or to impurities (λ_i). Hence, the total disappearance rate λ of the bound μp system in our H_2 -He-Ar mixtures can be written as

$$\lambda = \lambda_0 + \lambda_{pp} + \lambda_{pAr} + \lambda_{pHe} + \lambda_d + \lambda_i. \quad (5)$$

The different rates λ_x , excepting λ_0 , depend on the densities of the individual components and on the temperature. In order to compare such rates measured under different experimental conditions, they are reduced (normalized) to rates Λ_x corresponding to the atomic density of liquid hydrogen ($\rho_0 = 4.25 \times 10^{22} \text{ cm}^{-3}$). These reduced rates, which remain dependent on the collision energy of the μp atom with its partner, i.e., temperature dependent, are defined through

$$\lambda_x = c_x \frac{\rho}{\rho_0} \Lambda_x, \quad (6)$$

where c_x is the atomic concentration of element x, and ρ means the total atomic density of the investigated mixture. With Eq. (6), the total disappearance rate λ can then be written as

$$\lambda = \lambda_0 + \frac{\rho}{\rho_0} (c_p \Lambda_{pp} + c_{Ar} \Lambda_{pAr} + c_{He} \Lambda_{pHe} + c_d \Lambda_d + c_i \Lambda_i) . \quad (7)$$

If $N_0 \mu p$ atoms are formed at $t=0$, the number of μp systems $N_{\mu p}(t)$ still existing at time t is

$$N_{\mu p}(t) = N_0 e^{-\lambda t} . \quad (8)$$

The muonic deuterium atoms μd , which are essentially formed by muon transfer from μp atoms, can disappear by (a) free muon decay, (b) formation of $p\mu d$ molecules with a rate λ_{pd} , and (c) transfer of the muon to argon (λ_{dAr}), to helium (λ_{dHe}) or to impurities (λ'_i). In natural hydrogen, the direct capture of muons in deuterium and the formation of $d\mu d$ molecules are negligible. We can therefore write $N_{\mu d}(t=0)=0$, and $\lambda_{dd}=0$. The total number of μd atoms existing at time t must then satisfy the equation

$$\frac{dN_{\mu d}}{dt}(t) = \lambda_d N_{\mu p}(t) - \lambda' N_{\mu d}(t) , \quad (9)$$

with

$$\lambda' = \lambda_0 + \lambda_{pd} + \lambda_{dAr} + \lambda_{dHe} + \lambda'_i . \quad (10)$$

Part of the μp and μd atoms transfer their muon to highly excited states of argon. The time distribution of the promptly emitted muonic argon x rays is

$$\frac{dN_{\gamma Ar}}{dt}(t) = \lambda_{pAr} N_{\mu p}(t) + \lambda_{dAr} N_{\mu d}(t) . \quad (11)$$

For $t > 3\Gamma$, where Γ is the finite-time resolution of the detection system, and by using Eqs. (8) and (9), this time distribution can also be written as

$$\frac{dN_{\gamma Ar}}{dt}(t) \sim e^{-\lambda t} + \frac{\Lambda_{dAr}}{\Lambda_{pAr}} \frac{\lambda_d}{\lambda - \lambda'} (e^{-\lambda' t} - e^{-\lambda t}) . \quad (12)$$

This formula is only valid if the deexcitation to the ground state of $(\mu p)^*$ is very fast. The second term of formula (12), which is small compared to the first one, corresponds to transfer of muons from $(\mu d)_{1s}$ atoms to argon, and can be treated as a correction.

From the measured time distribution of the muonic argon x rays, $dN_{\gamma Ar}(t)/dt$, one extracts, by using formula (12), the reduced transfer rates Λ_{pAr} and Λ_{pHe} . The other rates of formulas (5) and (10) are known. The most recent experimental values of the reduced $p\mu p$ formation rate are consistent,³³⁻³⁵ the mean value being $\Lambda_{pp} = 2.5 \times 10^6 \text{ s}^{-1}$. The used values for Λ_d , Λ_{pd} , and Λ_{dHe} at room temperature are $1.68(26) \times 10^{10} \text{ s}^{-1}$ (Ref. 36), $5.53(16) \times 10^6 \text{ s}^{-1}$ (Ref. 35), and $3.68(18) \times 10^8 \text{ s}^{-1}$ (Ref. 21), respectively. If we would have taken other slightly different values for Λ_{pp} , Λ_d , and Λ_{pd} (Refs. 37 and 38), our final transfer rates would be changed by about 1%. We assume that the ratio $\Lambda_{pAr}/\Lambda_{dAr} = 2$, as measured for medium and high Z noble gases.^{39,40}

The transfer rate Λ_{pAr} is firstly measured in a binary H_2 -Ar mixture. With the known value for Λ_{pAr} , one then measures the transfer rate Λ_{pHe} in the ternary H_2 -He-Ar mixture.

IV. MEASUREMENT

For the measurement of the muon transfer to helium at low pressure (up to 15 atm), a special target vessel has been constructed (Fig. 2). It was made out of stainless steel with wall thicknesses of 2 mm. The flanges were equipped with copper sealings. The muon entrance window of 12 cm^2 in the center of the front flange was a thin steel foil ($50 \mu\text{m}$) or a capton foil ($120 \mu\text{m}$) supported by a copper grid which had a particle transmission of 90%. The vessel had a volume of 9 liters and could be evacuated by a turbomolecular pump to a final pressure of 10^{-8} mbar. By closing the valves, the pressure increased due to outgassing of the material and stabilized at about 10^{-2} mbar after a few hours.

The gas mixtures were directly ordered at the manufacturer.⁴¹ The purity of each component was better than 5 ppm and the precision of the concentrations $\pm 1\%$. The following gas mixtures were used for our measurements of the muon transfer at room temperature: (a) $\text{H}_2 + 0.408\% \text{ Ar}$ at 9.6 bar, (b) $\text{H}_2 + 1.98\% \text{ Ar}$ at 14.9 bar, (c) $\text{H}_2 + 649 \text{ ppm Ar} + 34.4\% \text{ He}$ at 14.8 bar, and (d) $\text{H}_2 + 943 \text{ ppm Ar} + 50.7\% \text{ He}$ at 14.8 bar. The concentrations are given as ratios of partial pressures to the total pressure of the mixture. Each mixture has been measured during 3-4 days. The pressure of the gas fluctuated by less than ± 0.1 bar and the temperature measured outside the vessel was $22(2)^\circ\text{C}$.

The experiment has been performed at the $\mu E4$ channel of the Swiss Institute for Nuclear Research (SIN), today the Paul Scherrer Institute (PSI). To optimize the muon capture in the gas mixture, muons of low momentum [30 or 32 MeV/c with a full width at half maximum (FWHM) of 3%] were directed onto the target. At 32 MeV/c, 2×10^4 muons/s passed the 0.5-mm-thick scintil-

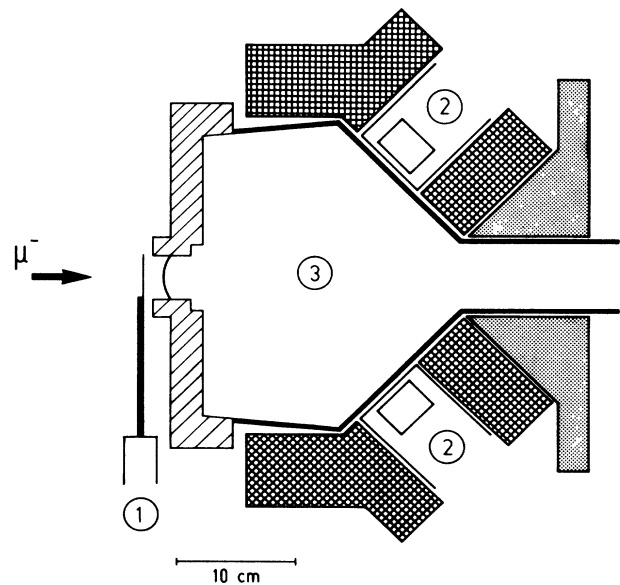


FIG. 2. Experimental setup: (1) scintillator, (2) Ge detectors, (3) gas vessel. Shielding: steel; lead; borated polyethylene.

lator, which yielded the start signal for the measurement.

The electronic setup was similar to that of the preceding experiment on muon transfer.⁹ An antipileup gate rejected those events, where a muon registered by the scintillator was preceded or followed by another muon in a time interval of 1 μ s in the H₂-Ar mixtures and 2 μ s in the triple gas mixtures. 10% of the muons were rejected on the average. The muonic x rays were registered by Ge semiconductor detectors. The first part of the measurements, (a)–(c), was performed using only one detector of 65 cm³ active volume. In the second part, (d), two detectors placed symmetrically relative to the muon beam were employed (Fig. 2), the second one with a volume of 98 cm³. The maximum load of the detectors was of the order of 2000 events per second. The time resolution Γ for the muonic Ar(2*p*–1*s*) x rays at 643 keV, measured in pure argon, was about 5 ns (FWHM).

The energy of the events was digitalized in 8-k channels and the time in 1-k channels with 0.75 ns/channel for the binary mixtures and 1.58 ns/channel for the triple ones. With the data acquisition program DAVID, the energy and time of the γ events were written in list mode on magnetic tape. Energy and time spectra were reconstructed offline for analysis.

V. DATA ANALYSIS

A. Transfer rates

Time spectra have been reconstructed by setting energy windows on the photopeaks of the muonic argon x rays and on the background on both sides of these peaks.

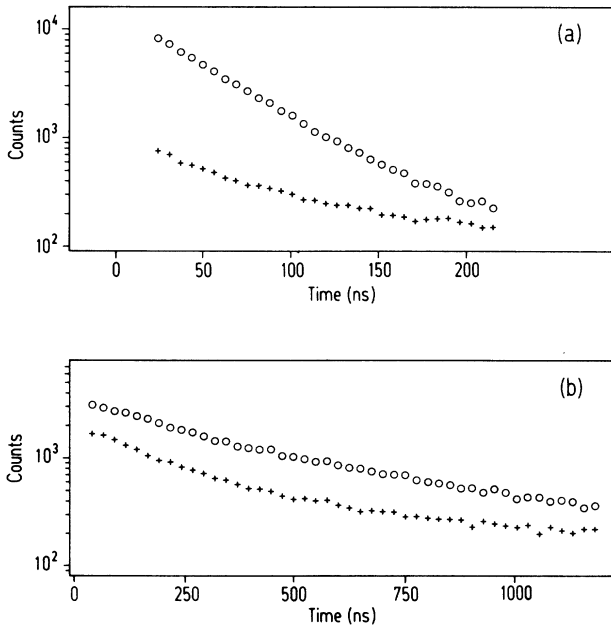


FIG. 3. Time distribution of the muonic Ar 2*p*-1*s* events (○) measured with the 65-cm³ Ge detector before subtraction of the background spectrum (+). The experimental errors are smaller than the sizes of the circles. Only the fitted domain is plotted. (a) H₂ + 1.98% Ar; (b) H₂ + 50.7% He + 943 ppm Ar.

As can be seen from Figs. 3(a) and 3(b), the time structures of the background events are different from those of the x-ray events. The net time spectrum of each transition was then obtained by subtracting the respective background time spectrum. The ratios of the net muonic argon 2*p*-1*s* events to the subtracted background events (for $t > 15$ ns) were 1.4, 5.7, 2.1, and 1.1 for the mixtures (a)–(d), respectively. Obviously, these ratios depend on the widths of the energy windows set on the 2*p*-1*s* peaks. In order to have all 2*p*-1*s* events in the time spectrum, the chosen widths were four times the FWHM. By choosing different energy windows for the background, the fitted time constants varied only in the limits of the statistical error.

The time distribution of the muonic argon x rays resulting from muons transferred from μp atoms is only slightly influenced by the muons transferred from μd atoms. The net time spectra can be fitted by using a single exponential [see Figs. 4(a) and 4(b)] with a time constant λ_{exp} , which is slightly lower than λ . The difference can be evaluated (see also Ref. 9). Equation (12) can be written as

$$e^{-\lambda t} + \frac{\Lambda_{dAr}}{\Lambda_{pAr}} \frac{\lambda_d}{\lambda - \lambda'} (e^{-\lambda' t} - e^{-\lambda t}) = e^{-\lambda_{\text{exp}} t}, \quad (13)$$

or as

$$e^{-\Delta\lambda t} = 1 - \frac{\Lambda_{dAr}}{\Lambda_{pAr}} \frac{\lambda_d}{\lambda_{\text{exp}} - \lambda'} (e^{(\lambda_{\text{exp}} - \lambda') t} - 1), \quad (14)$$

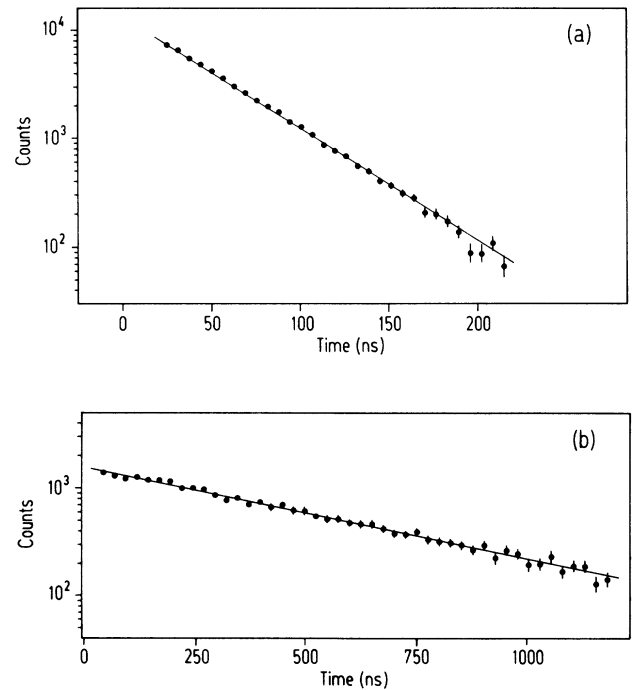


FIG. 4. Time distribution of the muonic Ar 2*p*-1*s* events measured with the 65-cm³ Ge detector after subtraction of the background. (a) H₂ + 1.98% Ar; (b) H₂ + 50.7% He + 943 ppm Ar.

where $\Delta\lambda = \lambda - \lambda_{\text{exp}}$ is the correction term due to muon transfer from μd atoms. The relative differences $\Delta\lambda/\lambda_{\text{exp}}$ for the mixtures (a)–(d) are then estimated to be 0.4%, 0.1%, 0.9%, and 0.5%, respectively. They are all smaller than the statistical errors on λ_{exp} .

The measured energy spectra extended up to about 1300 keV. In the time window corresponding to prompt events, these spectra contain also muonic iron x rays from muons stopped in the walls of the target vessel.

In the delayed energy spectra, no muonic x rays from nitrogen, oxygen, or other gaseous impurities are identified. Muonic iron x rays are again observed with intensities of a few percent as compared to the prompt spectra. However, they do not show the characteristic time structure of the argon events. In test measurements with pure argon, where no muon transfer occurs, the same flat time structure of iron x rays was found. We assume therefore that the largest part of the muonic iron x rays registered by measuring our hydrogen gas mixtures comes from muons stopped in front of the target entrance window in accidental coincidence with a stopped muon. By assuming as an upper limit for the gaseous impurities a partial pressure of 10^{-2} mbar, corresponding to the outgassing pressure, and a transfer rate of the order of $\Lambda_i = 10^{11} \text{ s}^{-1}$, the contribution of λ_i to λ in Eq. (5) remains negligible. In our data analysis, we have consequently neglected both the transfer to the target walls and to impurities contained in the gas mixtures.

For each gas mixture, the net time spectrum of the muonic $\text{Ar}(2p-1s)$ transition has been analyzed. In the $\text{H}_2 + 1.98\%$ Ar mixture, the 3-1 and 4-1 transitions had sufficient statistics, so that the analysis of their time structure can be used to improve the uncertainty in the transfer rate deduced from the 2-1 transition alone.

B. Intensities

The two figures 5(a) and 5(b) show energy spectra of the muonic Lyman series in argon taken in the two mixtures $\text{H}_2 + 1.98\%$ Ar and $\text{H}_2 + 34.4\%$ He + 649 ppm Ar. They have been formed by setting windows on the time spectra ($t > 20$ ns). The peak-to-background ratio was of the order of 8.

The exact determination of the intensities of the higher members of the muonic Lyman series transitions was rendered more difficult by the presence of background γ lines at 833.95 keV [$^{72}\text{Ge}(n, n')$], 846.78 keV [$^{56}\text{Fe}(n, n')$], and 858.3 keV. In particular, the intensity of the $\text{Ar}(6p-1s)$ transition, covered by the strong 846-keV line, could only be estimated from a measurement at high pressure.⁹ The efficiency calibration of the detection system has been performed using radioactive sources of ^{152}Eu and ^{182}Ta .⁴²

VI. RESULTS AND DISCUSSION

A. Transfer rates

The shapes of our delayed time spectra, with or without the presence of helium, are purely exponential [Figs. 4(a) and 4(b)]. This indicates that the μp atoms

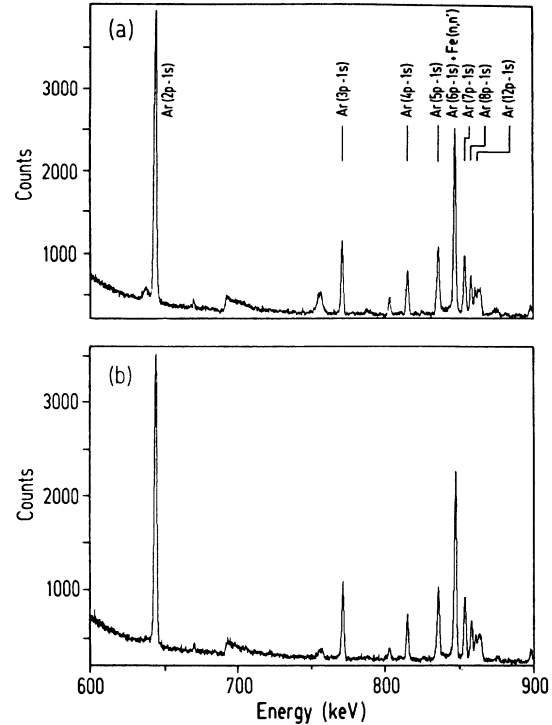


FIG. 5. Muonic Lyman series intensities in argon by muon transfer from μp atoms. (a) $\text{H}_2 + 1.98\%$ Ar; (b) $\text{H}_2 + 34.4\%$ He + 649 ppm Ar.

transferring their muon are in the ground states (singlet or triplet) and have thermal energies.

The measured lifetimes $\tau = 1/\lambda$ of the μp system in its ground state in the mixtures $\text{H}_2 + 0.408\%$ Ar and $\text{H}_2 + 1.98\%$ Ar and the deduced reduced transfer rates to argon, $\Lambda_{p\text{Ar}}$, are given in Table I. The uncertainties of these values include the uncertainties in the fit, the pressure, the gas concentrations, and the time calibration. While there are discrepancies with other authors, as can be seen from Table II, the measurements of our group at four different total pressures (9.6, 14.9, 100, and 140 bar) and four different argon concentrations (0.408%, 1.98%, 0.06%, and 0.2%) are in excellent agreement. A detailed comparison with the experimental values of other authors^{39,43–46} has already been made in our earlier paper.⁹ We have no explanation for the discrepancies between the reduced rates. Although the agreement between our four rates, measured under very different experimental conditions, does not prove that the transfer rate is strictly

TABLE I. Total μp lifetime and reduced transfer rate to argon at 295 K, measured in this work.

	$\text{H}_2 + 0.408\%$ Ar 9.6 bars	$\text{H}_2 + 1.98\%$ Ar 14.9 bars	Average value
$\tau = 1/\lambda$ (ns)	257(14)	40.1(14)	
$\Lambda_{p\text{Ar}}$ (10^{11} s^{-1})	1.48(8)	1.43(5)	1.44(4)

TABLE II. Comparative table of measured reduced transfer rates to argon at different pressures.

Authors	Pressure (bars)	$\Lambda_{pAr}(10^{11} \text{ s}^{-1})$
Basiladze <i>et al.</i> ^a	45	1.20(19)
Alberigi <i>et al.</i> ^b	26	3.48(60)
Placci <i>et al.</i> ^c	10	1.46(14)
Daniel <i>et al.</i> ^d	600	9.8(15)
Iacopini <i>et al.</i> ^e	2–4	3.67(72)
Bienz <i>et al.</i> ^f	100	1.42(16)
	140	1.46(5)
This work	9.6	1.48(8)
	14.9	1.43(5)

^aReference 43.^bReference 44.^cReference 39.^dReference 45.^eReference 46.^fReference 9.

proportional to the density of the gas admixed to hydrogen, it corroborates this assumption. For the determination of the transfer rate to helium using the triple gas method, we assume a strict proportionality to the density.

In our gas mixtures with high helium concentrations, the muon can transfer to helium from excited (μp)* states. The argon concentration however is so low that transfer to argon occurs only from μp ground state. By measuring in a H₂-He-Ar gas mixture the time distribution of the muonic argon x rays due to muon transfer, one measures the lifetime $\tau=1/\lambda$ of the μp ground state. Using Eqs. (7) and (14), and taking for the transfer rate to argon the value $\Lambda_{pAr}=1.44(4)\times 10^{11} \text{ s}^{-1}$, the reduced transfer rate to helium Λ_{pHe} from the ground state of the μp system can be determined. The rates Λ_{pHe} are listed in Table III. The results from the different measurements are in agreement with each other. In particular, changing the helium concentration by 50% does not alter the normalized rate.

Our mean value for Λ_{pHe} is higher than the experimental result by Bystritskii *et al.*¹⁷ (cf. Table IV). Their experimental conditions, i.e., pressure and helium concentration, are comparable to ours. They also used the triple gas method (with xenon instead of argon) and analyzed the time distribution of the photons. The experimental techniques and the analysis, however, differ in some points. While we utilize the photon time spectrum of a narrow energy window ($\Delta E \cong 7 \text{ keV}$) containing the muonic Ar($2p-1s$) events and subtract the time spectrum

TABLE IV. Comparative table of measured and predicted transfer rates to ⁴He at room temperature.

Author	Experiment $\Lambda_{pHe} (10^8 \text{ s}^{-1})$	Theory $\Lambda_{pHe} (10^8 \text{ s}^{-1})$
Aristov <i>et al.</i> ^a		0.44
Bystritskii <i>et al.</i> ^b	0.36(10)	
Kravtsov <i>et al.</i> ^c		0.43–0.52
Ivanov <i>et al.</i> ^d		0.32–0.35
This work	0.88(9)	

^aReference 16.^bReference 17.^cReference 18.^dReference 19.

of background photons adjacent to the line. Bystritskii *et al.* take a larger energy window and subtract the background photon time spectrum measured without xenon in the vessel. Depending on the argon density, our time spectra extended to a maximum of only 1.4 μs after a muon stop signal, whereas their time spectra had lengths of about 8 μs . Finally, we have made use of the measured value of the transfer rate to admixed third component, whereas Bystritskii *et al.* do not need the transfer rate to xenon to determine the transfer rate to helium.

Among the various theoretical approaches proposed to calculate the transfer rate to helium, the “thawed core” and the “frozen core” approaches of Ivanov *et al.*¹⁹ give predictions close to the experimental values for $\mu p + ^4\text{He}$ (Ref. 17), $\mu d + ^3\text{He}$ (Refs. 5 and 21), and $\mu t + ^3\text{He}$ (Ref. 5). However, they are significantly lower than the values of $\mu d + ^4\text{He}$ (Refs. 20 and 21) and our $\mu p + ^4\text{He}$ result.

B. Intensity patterns in muonic argon

The relative intensities of the muonic Lyman series in argon due to muon transfer have also been evaluated and are listed in Table V. As a check, the relative intensities have also been determined in different time windows of the delayed spectra. They show always the same pattern. No significant differences are found in the intensity structures between the mixtures with or without helium.

The relative intensities agree with those measured in a H₂-Ar mixture at a high pressure of 800 bar.⁴⁷ This demonstrates nicely that the muonic x-ray intensity structure in argon due to transfer from μp atoms is over a large range independent of pressure. Such a result is expected, since the μp atom penetrates inside the electron orbits of argon and transfers its muon to atomic levels

TABLE III. Total μp lifetime and reduced transfer rates to ⁴He at room temperature, measured in this work at a pressure of 14.8 bars, using $\Lambda_{pAr}=1.44(4)\times 10^{11} \text{ s}^{-1}$.

Ge detector	H ₂ + 50.7% He + 943 ppm Ar		H ₂ + 34.4% He + 649 ppm Ar	Average value
	65 cm ³	98 cm ³	65 cm ³	
$\tau=1/\lambda$ (ns)	496(10)	491(15)	633(10)	
Λ_{pHe} (10^8 s^{-1})	0.83(14)	0.88(15)	0.92(14)	0.88(9)

TABLE V. Normalized muonic x-ray intensities of the Lyman series in argon by transfer from protium.

Transition	H ₂ +0.408% Ar	H ₂ +1.98% Ar	H ₂ +50.7% He +943 ppm Ar	H ₂ +34.4% He +649 ppm Ar	Holzwarth ^a and MUON00 ^b
2-1	0.425(21)	0.391(9)	0.417(20)	0.390(10)	0.419
3-1	0.105(3)	0.100(2)	0.102(3)	0.102(2)	0.092
4-1	0.059(3)	0.064(2)	0.063(3)	0.063(2)	0.063
5-1	0.088(9)	0.095(2)	0.095(10)	0.095(6)	0.093
6-1	0.105	0.112	0.102	0.112	0.113
7-1	0.085(3)	0.089(2)	0.082(3)	0.090(2)	0.090
8-1	0.046(4)	0.046(3)	0.047(5)	0.046(3)	0.051

^aReference 53.^bReference 54.

around $n = 12$.⁴⁸ Geometrically, these orbits lie between the electronic K shell and the nucleus. The principal deexcitation modes are radiative transitions and K -shell Auger electron ejection in the presence of full higher electron shells. Thus, the refilling of electron holes through collisions with other atoms is not an essential process in the muon cascade. Contrary to capture by transfer, the direct muon capture occurs at very high n levels ($n = 30-40$), such that at low pressure the muonic atom can lose all its electrons during the cascade process.⁴⁹ In this case strong density effects are expected and have indeed been observed.⁵⁰⁻⁵²

Following Holzwarth and Pfeiffer,⁵³ the muon transferred to argon populates preferentially low angular momentum states. A cascade calculation using the code MUON00,⁵⁴ starting at the muonic level $n = 12$ with an angular momentum distribution predicted by Holzwarth and Pfeiffer, reproduces in a satisfactory manner the measured muonic x-ray intensities (Table V), assuming the electron shells to be complete when the muon is transferred.

VII. CONCLUSION

Our reduced transfer rates to argon, Λ_{pAr} , measured in H₂-Ar gas mixtures at low (10 and 15 bars) and at high (100 and 140 bars) pressures are the same and do not seem to depend on the argon concentration. They are,

however, in disagreement with most other experimental transfer rates excepting Refs. 39 and 43, where the decay electron method has been employed.

Our two independent measurements of the muon transfer rate from the μp ground state to helium, Λ_{pHe} , yield values in agreement with each other. They are, however, a factor of 2 higher than the experimental value of Bystritskii *et al.*¹⁷ and the different theoretical predictions.^{16,18,19} The reasons for these disagreements are not known. Taking for Λ_{pHe} the value of Bystritskii *et al.* and calculating Λ_{pAr} from our experimental μp disappearance rate λ measured in the two H₂-He-Ar mixtures (Table III), one obtains for both mixtures $\Lambda_{pAr} \cong 1.7 \times 10^{11} \text{ s}^{-1}$. This value is also in disagreement with all other experimental values (Table II).

Finally, our measured muonic x-ray intensities of the Lyman series of argon resulting from muon transfer are independent of pressure and argon concentration. They are not affected by the presence of helium and agree well with theoretically predicted intensities.

ACKNOWLEDGMENTS

The authors thank Dr. P. Bergem, D. Siradovic, and H. Tschopp for their help in the design and construction of the gas target. They appreciate the financial support of the Swiss National Science Foundation and PSI.

¹L. W. Alvarez, H. Bradner, F. S. Crawford, Jr., J. A. Crawford, P. Falk-Vairant, M. L. Good, J. D. Gow, A. H. Rosenfeld, F. Solmitz, M. L. Stevenson, H. K. Ticho, and R. D. Tripp, *Phys. Rev.* **105**, 1127 (1957).

²V. M. Bystritskii, V. P. Dzhelepov, V. I. Petrukhin, A. I. Rudenko, L. N. Somov, V. M. Suvorov, V. V. Fil'chenkov, G. Hemnitz, N. N. Khovanskii, B. A. Khomenko, and D. Horvath, *Zh. Eksp. Teor. Fiz.* **76**, 460 (1979) [*Sov. Phys.—JETP* **49**, 232 (1979)].

³Yu. V. Petrov, *Nature* **285**, 466 (1980); S. G. Lie and A. A. Harms, *Nucl. Sci. Eng.* **80**, 124 (1982); A. Kumar and S. Sahin, *Trans. Am. Nucl. Soc.* **43**, 217 (1982).

⁴D. V. Balin, E. M. Maev, V. I. Medvedev, G. G. Semenchuk, Yu. V. Smirenin, A. A. Vorobyov, An. A. Vorobyov, and Yu. K. Zalite, *Phys. Lett.* **B141**, 173 (1984).

⁵S. E. Jones, A. N. Anderson, A. J. Caffrey, J. B. Walter, K. D. Watts, J. N. Bradbury, P. A. M. Gram, M. Leon, H. R. Maltrud, and M. A. Paciotti, *Phys. Rev. Lett.* **51**, 1757 (1983).

⁶W. H. Breunlich, M. Cargnelli, P. Kammel, J. Marton, N. Naegele, P. Pawlek, A. Scrinzi, J. Werner, J. Zmeskal, J. Bistirlich, K. M. Crowe, M. Justice, J. Kurck, C. Petitjean, R. H. Sherman, H. Bossy, H. Daniel, F. J. Hartmann, W. Neumann, and G. Schmidt, *Phys. Rev. Lett.* **58**, 329 (1987).

⁷K. Nagamine, T. Matsuzaki, K. Ishida, Y. Hirata, Y. Watanabe, R. Kadono, Y. Miyake, K. Nishiyama, S. E. Jones, and H. R. Maltrud, *Muon Catalyzed Fusion* **1**, 137 (1987).

⁸S. S. Gershtein, and L. I. Ponomarev, *Phys. Lett.* **B72**, 80 (1977).

⁹F. Bienz, P. Bergem, M. Boschung, R. Jacot-Guillarmod, G.

- Piller, W. Reichart, L. A. Schaller, L. Schellenberg, H. Schneuwly, and G. Torelli, *J. Phys. B* **21**, 2725 (1988).
- ¹⁰M. Schiff, *Nuovo Cimento* **22**, 66 (1961).
- ¹¹O. A. Zaimidoroga, M. M. Kulyukin, R. M. Sulyaev, A. I. Filippov, V. M. Tsupkositnikov, and Y. A. Shcherbakov, *Zh. Eksp. Teor. Fiz.* **44**, 1852 (1963) [*Sov. Phys.—JETP* **17**, 1246 (1963)].
- ¹²A. Placci, E. Zavattini, A. Bertin, and A. Vitale, *Nuovo Cimento A* **52**, 1274 (1967).
- ¹³A. Bertin, A. Vitale, and E. Zavattini, *Lett. Nuovo Cimento* **18**, 381 (1977).
- ¹⁴S. S. Gershtein, *Zh. Eksp. Teor. Fiz.* **43**, 706 (1962) [*Sov. Phys.—JETP* **16**, 501 (1963)].
- ¹⁵A. V. Matveenko and L. I. Ponomarev, *Zh. Eksp. Teor. Fiz.* **63**, 48 (1972) [*Sov. Phys.—JETP* **36**, 24 (1973)].
- ¹⁶Yu. A. Aristov, A. V. Kravtsov, N. P. Popov, G. E. Solyakin, N. F. Truskova, and M. P. Faifman, *Sov. J. Nucl. Phys.* **33**, 564 (1981).
- ¹⁷V. M. Bystritskii, V. P. Dzhelepov, V. I. Petrukhin, A. I. Rudenko, V. M. Suvorov, V. V. Filchenkov, N. N. Khovanskii, and B. A. Khomenko, *Zh. Eksp. Teor. Fiz.* **84**, 7257 (1983) [*Sov. Phys.—JETP* **57**, 728 (1983)].
- ¹⁸A. V. Kravtsov, A. I. Mikhailov, and N. P. Popov, *J. Phys. B* **19**, 2579 (1986).
- ¹⁹V. K. Ivanov, A. V. Kravtsov, A. I. Mikhailov, N. P. Popov, and V. I. Fomichev, *Zh. Eksp. Teor. Fiz.* **91**, 358 (1986) [*Sov. Phys.—JETP* **64**, 210 (1986)].
- ²⁰T. Matsuzaki, K. Ishida, K. Nagamine, Y. Hirata, and R. Kadono, *Muon Catalyzed Fusion* **2**, 217 (1988).
- ²¹D. V. Balin, A. A. Vorob'ev, An. A. Vorob'ev, Yu. K. Zalite, A. A. Markov, V. I. Medvedev, E. M. Maev, G. G. Semenchuk, and Yu. V. Smirenin, *Pis'ma Zh. Eksp. Teor. Fiz.* **42**, 236 (1985) [*JETP Lett* **42**, 293 (1985)].
- ²²A. Bertin, I. Massa, M. Piccinini, A. Vacchi, G. Vannini, and A. Vitale, *Phys. Lett.* **B78**, 355 (1978).
- ²³A. Alberigi Quaranta, A. Bertin, G. Matone, F. Palmonari, A. Placci, P. Dalpiaz, G. Torelli, and E. Zavattini, *Phys. Rev.* **177**, 2118 (1969).
- ²⁴J. F. Crawford, M. Daum, R. Frosch, B. Jost, P.-R. Kettle, R. M. Marshall, B. K. Wright, and K. O. H. Ziock, *Paul Scherrer Institute Report No. PR-88-05*, 1988 (unpublished).
- ²⁵V. E. Markushin, *Zh. Eksp. Teor. Fiz.* **80**, 35 (1981) [*Sov. Phys.—JETP* **53**, 16 (1981)].
- ²⁶A. V. Kravtsov, N. P. Popov, G. E. Solyakin, Yu. A. Aristov, M. P. Faifman, and N. F. Truskova, *Phys. Lett.* **A83**, 379 (1981).
- ²⁷A. Bertin, M. Capponi, I. Massa, M. Piccinini, G. Vannini, M. Poli, and A. Vitale, *Nuovo Cimento A* **72**, 225 (1982).
- ²⁸V. S. Melezhik, L. I. Ponomarev, and M. P. Faifman, *Zh. Eksp. Teor. Fiz.* **85**, 434 (1983) [*Sov. Phys.—JETP* **58**, 254 (1983)].
- ²⁹L. I. Ponomarev, L. N. Somov, and M. P. Faifman, *Yad. Fiz.* **29**, 133 (1979) [*Sov. J. Nucl. Phys.* **29**, 67 (1979)].
- ³⁰A. V. Matveenko and L. I. Ponomarev, *Zh. Eksp. Teor. Fiz.* **53**, 1593 (1970) [*Sov. Phys.—JETP* **32**, 871 (1971)].
- ³¹P. Kammel, *Lett. Nuovo Cimento* **43**, 349 (1985).
- ³²V. I. Petrukhin and V. M. Suvorov, *Zh. Eksp. Teor. Fiz.* **70**, 1145 (1976) [*Sov. Phys.—JETP* **43**, 595 (1976)].
- ³³G. Conforto, C. Rubbia, E. Zavattini, and S. Focardi, *Nuovo Cimento* **33**, 1001 (1964).
- ³⁴Yu. G. Budyashov, P. F. Ermolov, V. G. Zinov, A. D. Konin, A. I. Mukhin, and K. O. Oganessian, *Joint Institute for Nuclear Research Report No. P15-3964*, 1968 (unpublished).
- ³⁵V. M. Bystritskii, V. P. Dzhelepov, V. I. Petrukhin, A. I. Rudenko, V. M. Suvorov, V. V. Fil'chenkov, G. Khemnits, N. N. Khovanskii, and B. A. Khomenko, *Zh. Eksp. Teor. Fiz.* **70**, 1167 (1976) [*Sov. Phys.—JETP* **43**, 606 (1976)].
- ³⁶A. Bertin, M. Bruno, A. Vitale, A. Placci, and E. Zavattini, *Lett. Nuovo Cimento* **4**, 449 (1972).
- ³⁷E. J. Bleser, E. W. Anderson, L. M. Ledermann, S. L. Meyer, J. L. Rosen, J. E. Rothberg, and I-T. Wang, *Phys. Rev.* **132**, 2679 (1963).
- ³⁸W. H. Bertl, W. H. Breunlich, P. Kammel, H. G. Mahler, W. L. Reiter, W. J. Kossler, L. A. Schaller, L. Schellenberg, and C. Petitjean, *Atomkernenergie* **43**, 184 (1983).
- ³⁹A. Placci, E. Zavattini, A. Bertin, and A. Vitale, *Nuovo Cimento A* **64**, 1053 (1969).
- ⁴⁰A. Bertin, M. Bruno, A. Vitale, A. Placci, and E. Zavattini, *Phys. Rev. A* **7**, 462 (1973).
- ⁴¹Carbagas SA, CH-3097 Liebefeld-Bern, Switzerland.
- ⁴²National Council on Radiation Protection and Measurements Report No. 58, 1985 (unpublished).
- ⁴³S. G. Basiladze, P. F. Ermolov, and K. O. Oganessian, *Zh. Eksp. Teor. Fiz.* **49**, 1042 (1965) [*Sov. Phys.—JETP* **22**, 725 (1966)].
- ⁴⁴A. Alberigi Quaranta, A. Bertin, G. Matone, F. Palmonari, A. Placci, P. Dalpiaz, G. Torelli, and E. Zavattini, *Nuovo Cimento B* **42**, 236 (1967).
- ⁴⁵H. Daniel, H.-J. Pfeiffer, P. Stoeckel, T. von Egidy, and H. P. Povel, *Nucl. Phys. A* **345**, 409 (1980).
- ⁴⁶E. Iacopini, G. Carboni, G. Torelli and V. Trobbiani, *Nuovo Cimento A* **67**, 201 (1982).
- ⁴⁷H.-J. Pfeiffer, K. Springer, and H. Daniel, *Nucl. Phys. A* **254**, 433 (1975).
- ⁴⁸G. Fiorentini and G. Torelli, *Nuovo Cimento A* **36**, 317 (1976).
- ⁴⁹R. Bacher, D. Gotta, L. M. Simons, J. Missimer, and N. C. Mukhopadhyay, *Phys. Rev. Lett.* **54**, 2087 (1985).
- ⁵⁰J. P. Knight, C. J. Orth, M. E. Schillaci, R. A. Naumann, F. J. Hartmann, and H. Schneuwly, *Phys. Rev. A* **27**, 2936 (1983).
- ⁵¹P. Ehrhart, F. J. Hartmann, E. Köhler, and H. Daniel, *Z. Phys. A* **311**, 259 (1983).
- ⁵²R. Jacot-Guillarmod, F. Bienz, M. Boschung, C. Piller, L. A. Schaller, L. Schellenberg, H. Schneuwly, and D. Siradovic, *Phys. Rev. A* **37**, 3795 (1988).
- ⁵³G. Holzwarth, and H.-J. Pfeiffer, *Z. Phys. A* **272**, 311 (1975).
- ⁵⁴V. R. Akylas, and P. Vogel, *Comp. Phys. Commun.* **15**, 291 (1978).

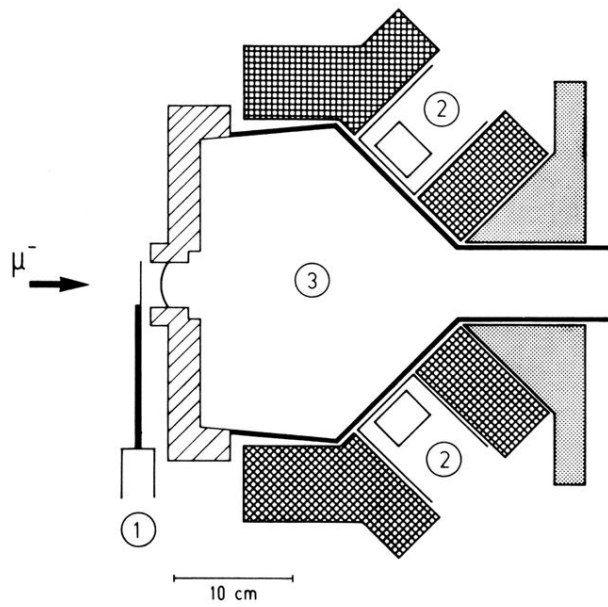
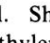
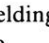
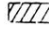


FIG. 2. Experimental setup: (1) scintillator, (2) Ge detectors, (3) gas vessel. Shielding: , steel; , lead; , borated polyethylene.